DAHLGREN DIVISION
NAVAL SURFACE WARFARE CENTER
Dahlgren, Virginia 22448-5100

NSWCDD/TR-97/144

SOUND INTENSITY PREDICTION SYSTEM (SIPS): VOLUME I—REFERENCE MANUAL

BY MICHEAL M. KORDICH DEAN A. POLLET

WEAPONS SYSTEMS DEPARTMENT

DECEMBER 1997

Approved for public release; distribution is unlimited.

REPORT DOCUMENTATION PAGE

Form Approved
OMB No. 0704-0188

1. AGENCY USE ONLY (Leave blank)

2. REPORT DATE

December 1997

3. REPORT TYPE AND DATES COVERED

Final

4. TITLE AND SUBTITLE

Sound Intensity Prediction System (SIPS): Volume I—Reference Manual

5. FUNDING NUMBERS

6. AUTHOR(s)

Micheal M. Kordich, Dean A. Pollet

7. PERFORMING ORGANIZATION NAME(S) AND ADDRESS(ES)

Commander
Naval Surface Warfare Center
Dahlgren Division (Code G72)
17320 Dahlgren Road
Dahlgren, VA 22448-5100

8. PERFORMING ORGANIZATION REPORT NUMBER

NSWCDD/TR-97/144

9. SPONSORING/MONITORING AGENCY NAME(S) AND ADDRESS(ES)

10. SPONSORING/MONITORING AGENCY REPORT NUMBER

11. SUPPLEMENTARY NOTES

12a. DISTRIBUTION/AVAILABILITY STATEMENT

Approved for public release; distribution is unlimited.

12b. DISTRIBUTION CODE

13. ABSTRACT (Maximum 200 words)

The Sound Intensity Prediction System (SIPS) is a tool employed to reduce the number of complaints about noise from explosive operations. SIPS combines procedures for conducting explosive operations with an acoustic ray-tracing computer code to determine the locations of both noise enhancements and noise reductions. The program has been in use at Naval Surface Warfare Center, Dahlgren Division (NSWCDD) since 1975, and at other DoD installations as well.

By predicting areas that can expect either increased or decreased noise levels, noise levels in sensitive areas can be determined. Predictions of quiet zones covering those areas indicate the best times to schedule explosive events.

This report documents the theory behind SIPS as well as the program's evolutionary process. The different computer models that make predictions about sound distribution are approximately equivalent in their predictive power with different methods of getting results and displaying the output. The quality of SIPS predictions is enhanced by using the model only on days when the weather is stable. In addition, predictions of focusing should be considered as areas rather than points since there is a tendency for them to drift.

14. SUBJECT TERMS

Sound Intensity Prediction System (SIPS), sound propagation, Sonic Detection and Ranging Device (SODAR), ray tracing, BRL model, Schomer model

15. NUMBER OF PAGES

35

16. PRICE CODE

17. SECURITY CLASSIFICATION OF REPORTS	18. SECURITY CLASSIFICATION OF THIS PAGE	19. SECURITY CLASSIFICATION OF ABSTRACT	20. LIMITATION OF ABSTRACT
UNCLASSIFIED	UNCLASSIFIED	UNCLASSIFIED	UL

NSN 7540-01-280-5500

Standard Form 298 (Rev 2-89)
Prescribed by ANSI std. Z39-18
298-102

FOREWORD

The Sound Intensity Prediction System (SIPS) is a tool employed to reduce the number of complaints about noise from explosive operations. The work discussed in this report was conducted by the Weapons Integration and Technology Branch (G72) of the Combat Systems Safety and Engineering Division (G70). This project was funded by the Strategic Systems Program as a portion of the Poseidon C-3 second-stage rocket motor disposal operation at the Utah Test and Training Range, Hill Air Force Base in Ogden, Utah.

The authors would like to thank Dr. Philemon Chan of Jaycor Corporation and Michael M. Swisdak, Jr. of the Naval Surface Warfare Center, Indian Head Division, for reviewing this document for technical accuracy.

This report has been reviewed and approved for release by Joseph C. Monolo, Head Weapons Integration and Technology Branch, and Gary C. Blount, Head, Combat Systems Safety and Engineering Division.

Approved by:

DAVID S. MALYEVAC, Deputy Head
Weapons Systems Department

CONTENTS

ILLUSTRATIONS

1.0 INTRODUCTION

The Sound Intensity Prediction System (SIPS) is an acoustic ray tracing computer code to determine the locations of both noise enhancements and noise reductions from the conduct of explosive operations. Dr. N. H. Gholson developed the computer code, Reference 1, and Dr. L. L. Pater provided a set of operational procedures for program interpretation, Reference 2. The computer code was developed to manage noise generated by explosive operations at the Naval Surface Warfare Center, Dahlgren Division (NSWCDD) in Dahlgren, Virginia.

During the mid-1970s, the majority of explosive operations at NSWCDD involved gunfire on the Potomac River range. These firings included all guns within the Naval inventory up to the 16-inch/50-caliber and experimental ordnance being evaluated for Naval use. In addition to the river range, open-air explosive charges up to a maximum of 1,000 pounds of TNT are conducted at the Explosive Experimental Area.

NSWCDD was established at Dahlgren because of its rural location. With a small population, many of whom were employed by NSWCDD, explosive operations could be conducted on a production basis without regard to atmospheric conditions or time of day. Operations could begin at dawn and extend into darkness as long as there were no safety impacts. This philosophy served projects well until the population began to increase and NSWCDD became concerned that noise from explosive operations should not have an impact on the surrounding community. In an effort to control any noise impact, NSWCDD sought a tool to determine where the noise from its operations was going. This effort resulted in the development of SIPS, and in 1975 the program was implemented and its use mandated for all explosive operations.

SIPS has also been implemented at Department of Defense (DOD) installations other than NSWCDD, and it has been used as the basis of other noise propagation models. This report, Volume I, documents the theory and history of the SIPS program. Volume II provides an in-depth users manual for SIPS.

2.0 METEOROLOGICAL EFFECTS ON SOUND

The relationship between atmospheric conditions and sound intensity distribution was recognized as early as 1906, when a paper to the Royal Society of London described an area of silence during cannon fire for the funeral of Queen Victoria. This phenomenon was explained as the refraction of sound energy by the atmosphere, and many other papers were published on the subject. Beginning in this period, there was optimism that very accurate predictions of sound intensities and locations would be available when technology provided detailed, timely atmospheric information and fast computing devices. The prospect of more accurate predictions through advanced technology still holds today. If the amount and location of refracted sound energy can be predicted, explosive events can be conducted when the atmosphere directs most of the sound energy upward or to some neutral ground where it would exert no impact. Atmospheric refraction, therefore, offers a solution to noise control. If it did not exist, measures designed to decrease the energy released from explosive events could be more expensive and more problematic than monitoring the atmosphere.

Atmospheric refraction of sound energy is a function of sound velocity (V) with respect to altitude above the ground. If there were no weather effects and V remained constant with altitude, there would be no refraction, and pure spherical expansion of the energy would occur. This relationship is shown in Figure 1.

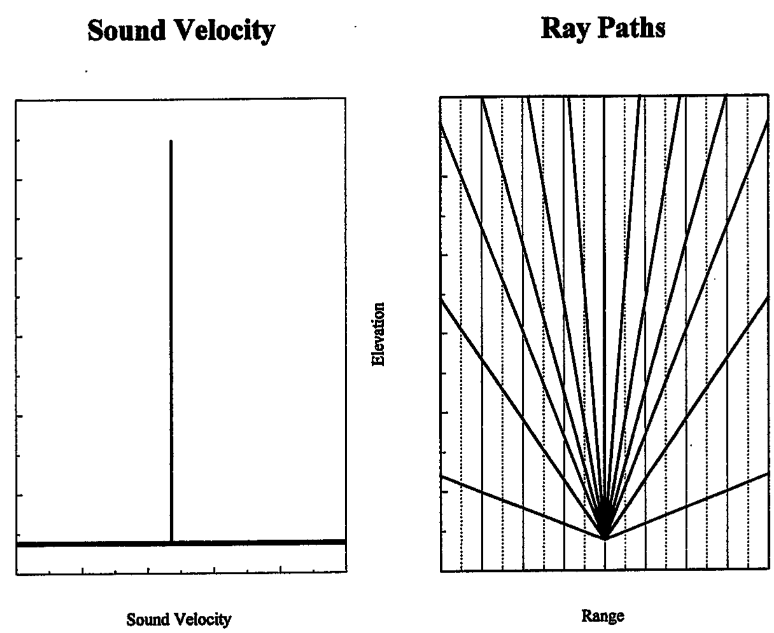

FIGURE 1. SOUND PROPAGATION IN ISOTHERMAL, STILL AIR

The speed of sound is a function of two physical parameters: air temperature and wind velocity. Humidity and air density have a less-than-1-percent influence; therefore, the effects of humidity and air density can be ignored. The general equation for the speed of sound in moving air in the horizontal direction is as follows:

$$V = V_o * [1 + T/273.15]^{1/2} - W_s * COS(\varphi - W_d) \quad (1)$$

where

V	= Total speed of sound in the φ direction	(ft/sec)
φ	= Direction of interest; measured clockwise from true north	(deg)
V_o	= Speed of sound in air at 0 °C (1087.53)	(ft/sec)
T	= Air temperature	(°C)
W_s	= Wind speed	(ft/sec)
W_d	= Wind origin direction; measured clockwise from true north	(deg)

As seen in Equation (1), the speed of sound is a square-root function of the air temperature in degrees Celsius. Two cases show the relationship between temperature lapse rate and speed of sound with no wind effects. The first case employs the U.S. Standard Atmosphere, Reference 3, that depicts an average temperature lapse rate, for nonrising air, of –3.56 °F (–1.98 °C) per 1000-ft increase in altitude. This decrease in temperature reflects a corresponding lapse rate for the sound speed of –3.94 ft/sec per 1000 ft. A decreasing sound speed refracts or bends the sound energy upward, where it is expended in the atmosphere, as illustrated in Figure 2.

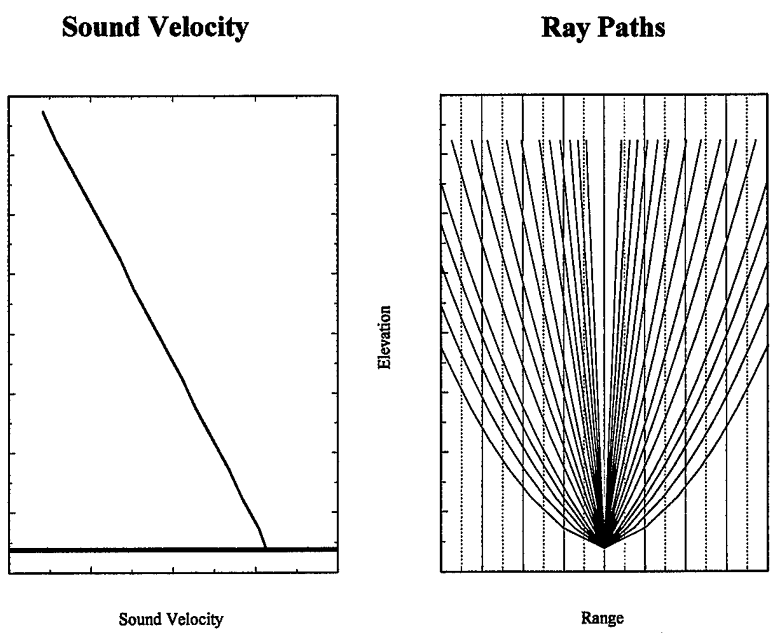

FIGURE 2. SOUND PROPAGATION FOR CONSTANTLY DECREASING SOUND VELOCITY IN STILL AIR

The second case employs the inverse of the U.S. Standard Atmosphere depicting an average temperature lapse rate of 3.56 °F (1.98 °C) per 1000-ft increase in altitude. This increase in temperature reflects a corresponding lapse rate for the sound speed of 3.94 ft/sec per 1000 ft. An increasing sound speed refracts or bends the sound energy downward, returning more sound energy to earth and resulting in elevated noise levels when compared to spherical expansion; see the illustration in Figure 3.

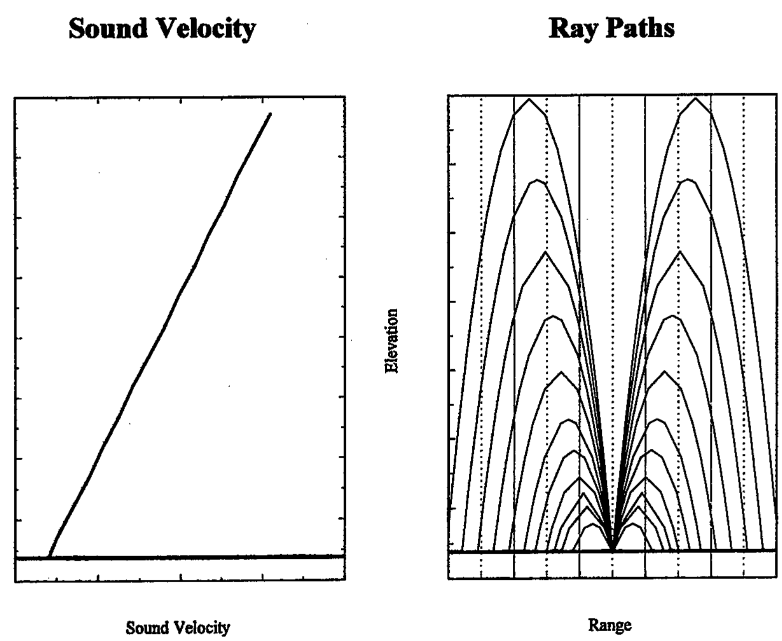

FIGURE 3. SOUND PROPAGATION FOR CONSTANTLY INCREASING SOUND VELOCITY IN STILL AIR

The wind component of Equation (1) can have a larger impact than temperature on sound speed. The magnitude of the wind component is dependent on the angle between the direction of interest and the direction of wind origin. This phase angle can be computed utilizing either φ or W_d as the lead term, inasmuch as the cosine function of Equation (1) is symmetrical about 0 deg; see Figure 4.

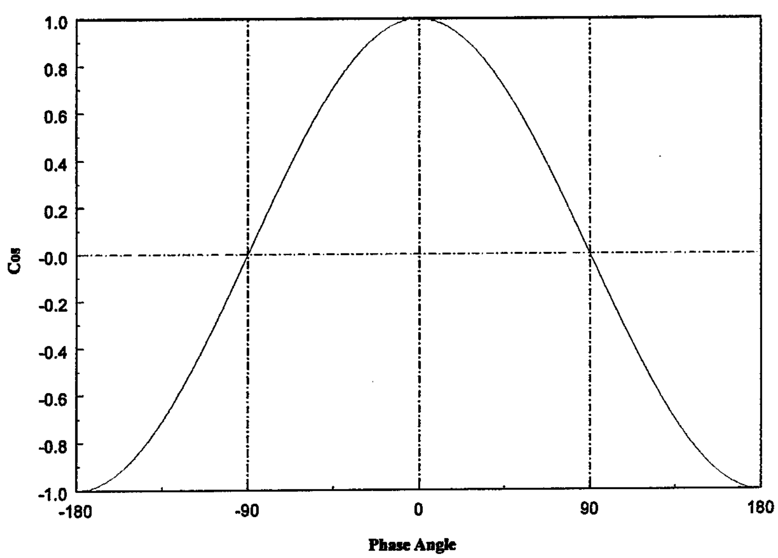

FIGURE 4. COSINE FUNCTION FOR PHASE ANGLE BETWEEN –180 AND 180 DEG

A decrease in sound speed occurs when there is a headwind with respect to the direction of interest. This condition depicts a phase angle with an absolute value between zero and 90 deg. The speed of sound increases, however, when the absolute value of the phase angle is between 90 and 180 deg, depicting a tail wind. A tail wind creates an adverse condition in that more sound energy is steered in the direction of interest. The effect of wind on sound energy is interesting in that if a certain direction has an intensification, the opposite direction has a comparable reduction. This phenomenon is shown in Figure 5.

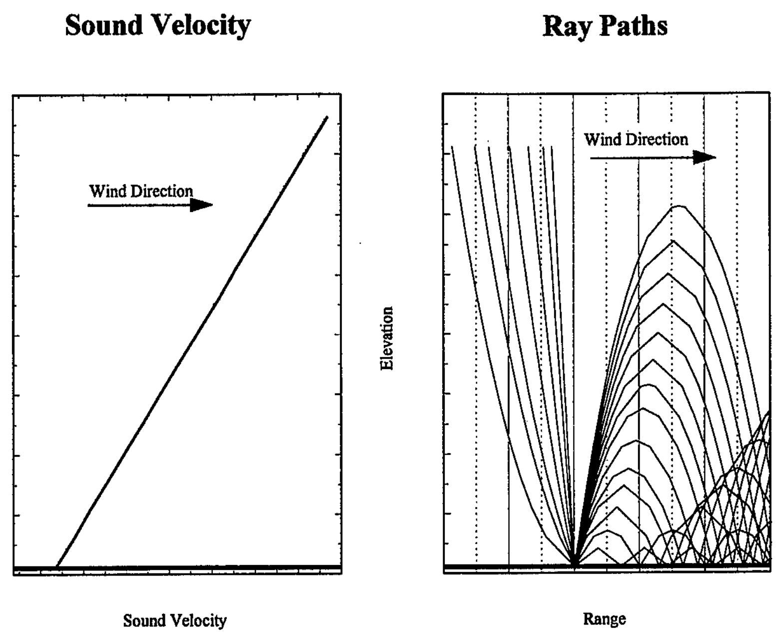

FIGURE 5. SOUND PROPAGATION FOR CONSTANTLY INCREASING WINDS, ISOTHERMAL

The preceding figures depict the simplest of sound velocity profiles in that all the profiles contain a single layer only. In reality, sound velocity profiles contain multiple layers governed by temperature inversions and wind shears. To illustrate this fact, an actual sound velocity profile and corresponding ray return paths from the Utah Test and Training Range (UTTR) are included as Figure 6. Figure 6 shows that there can be more than one level, which causes the sound rays to be refracted back to earth such that focusing can occur. The sound ray angle-of-departure from the explosion source governs which environmental factors affect the propagation. As the departure angle increases, the level at which the atmosphere affects the ray also increases. When the angle of departure becomes great enough, the atmosphere can no longer refract the sound rays downward, and they escape into the upper atmosphere. The subject of angle of departure is discussed in detail in the next chapter of this report.

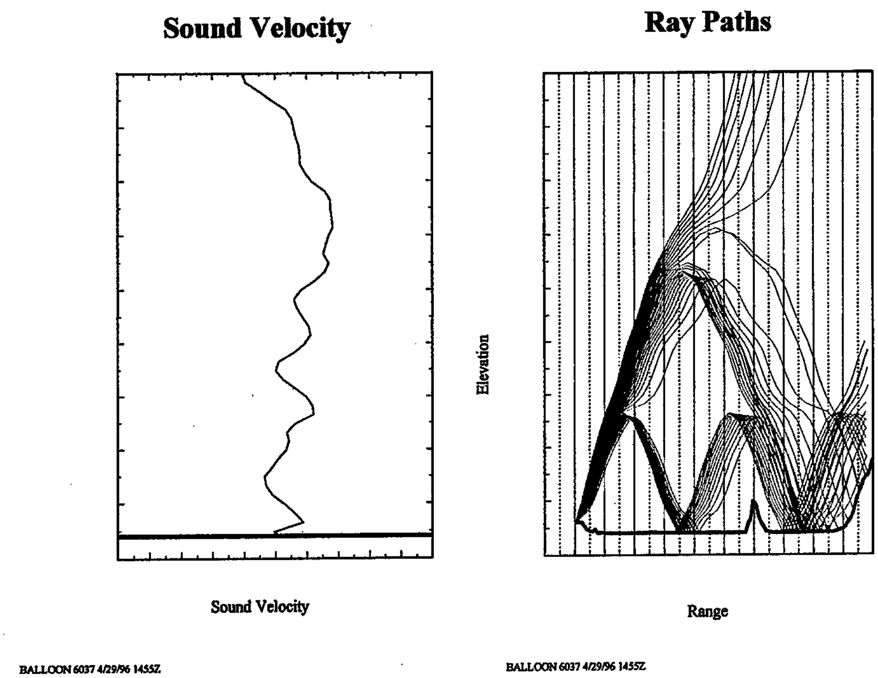

FIGURE 6. SOUND PROPAGATION FOR ACTUAL WEATHER CONDITIONS AT UTTR

Monitoring atmospheric conditions involves a meteorological data collection system employing either radiosondes or Sonic Detection And Ranging Device (SODAR) technology to collect the upper air parameters. Radiosondes are carried aloft by helium-filled balloons so that the scalar quantities of wet- and dry-bulb temperatures as well as atmospheric pressure can be retrieved. Since the balloon rides along with the wind, systems such as radio-navigation LORAN-C or Global Positioning System (GPS) must be employed to determine the balloon's location as a function of time and subsequently render the upper air wind speed and direction as a function of altitude. SODAR, the newest technology to furnish atmospheric data, has the advantage of less time between atmosphere soundings and describes the atmosphere directly above the unit, rather than at the balloon's location. The technology appears to be mature in terms of wind monitoring; but at present, SODAR is not capable of determining the air temperature at altitudes greater than approximately 20,000 ft. Upon retrieval of the two physical parameters, a model of the atmosphere is created as a series of stratified layers with constant horizontal properties. Each layer of the model represents a different linear sound-speed gradient.

3.0 SIPS PROGRAM THEORY

SIPS was developed in the early 1970s by Dr. N. H. Gholson, who employed the ray-tracing techniques documented in Reference 4. Ray tracing is a mature, labor-intensive method for determining the propagation of optical or acoustic energy through a medium considering only the geometrical aspects of the propagation. Spectral characteristics of the energy are not considered. The frequency content of the energy is defined as all-inclusive with zero wavelength, so that the wave can be treated as a line. Ray paths are defined as lines normal to the expanding propagation surface, each part of which expands at the speed of sound determined by the local properties of the medium. The current availability of fast computers with large amounts of memory makes ray tracing a viable technique in the analysis of sound propagation in the atmosphere.

3.1 RAY PATH THEORY

The ray paths as traced through the atmosphere obey Snell's Law. The angle of inclination from horizontal (θ) of the ray along with the sound speed (**V**), a function of altitude, determines a constant, $\delta = \mathbf{cos}\ (\theta)\ /\ \mathbf{V}$, at any point along that path. Each ray departing the sound's origin is associated with a unique constant set by the initial angle of departure θ_o, since all rays have the same initial sound speed, $\mathbf{V_o}$. If the ray is refracted downward, because of encountering a turning point velocity $\mathbf{V_{TP}}$ such that $\mathbf{V_{TP}} > \mathbf{V_o}$, and θ goes to 0 ($\cos(\theta) = 1$), then:

$$\delta = \mathbf{cos}\ (\theta_o) / \mathbf{V_o} = \mathbf{cos}\ (\theta) / \mathbf{V} = \mathbf{1} / \mathbf{V_{TP}} \tag{2}$$

Once $\mathbf{V_{TP}}$ is determined from the weather data, the maximum angle of departure (θ_{MAX}) for a ray can be found by substitution into Equation (2) as:

$$\theta_{MAX} = \mathbf{cos}^{-1}\ (\mathbf{V_o} / \mathbf{V_{TP}}) \tag{3}$$

θ_{MAX} is the dividing point beyond which rays with a larger angle of departure would never refract downward. Conversely, an angle of departure less than θ_{MAX} will refract downward when it reaches its unique $\mathbf{V_{TP}}$. If $\mathbf{V_o}$ is greater than any sound speed aloft, acoustic rays will never return to the ground even when $\theta_o = 0$. SIPS defines this situation as a quiet zone and performs no ray-tracing calculations.

The total speed of sound (**V**) in the atmosphere was defined in Equation (1) as a function of air temperature and directed wind velocity. Because Snell's law was never derived for a moving medium (Reference 5), an approximation in the way the wind speed, $\mathbf{W_S}$, is added to the temperature-dependent part of the sound speed, $\mathbf{V_T}$, was introduced. The relationship $\mathbf{V} = \mathbf{V_T} + \mathbf{W_S}$, used in SIPS, is sufficiently accurate as long as the ray's angle of inclination is small and the wind speed is not a large percentage of the total sound speed. The value of θ, in practice, is rarely greater than 10 deg and is usually less than 5 deg. The complete treatment of acoustic ray propagation in the atmosphere is given in Reference 6, which is a comprehensive theoretical development, rather than a guide to numerical techniques.

If the atmosphere was a stationary medium, sound propagation would occur symmetrically about the source, and rays traced in any direction would look alike, as shown in Figures 1 through 3. Because of the wind, it becomes necessary to select directions of interest and account for the wind speed component in those directions when calculating ray paths. The sound speed profile for each direction of interest represents a two-dimensional plane about ground zero (GZ). Calculations proceed one-plane-at-a-time until a 360 deg sweep defines the full pattern of noise distribution. This piecemeal approach keeps ray path computations and focus detection algorithms simple. Reference 5 states that such an approach is adequate, but a three-dimensional technique is no longer excessively computational. The three-dimensional approach would include cross wind effects, such that the ray's path can also undergo an azimuth change. Three-dimensional techniques are being investigated as part of the ongoing effort for improving SIPS.

The atmospheric parameters needed as input to SIPS are collected by a single atmospheric sounding as near as possible to the noise event site. These parameters are considered valid for approximately one hour. Such a sampling technique suggests that the atmosphere be modeled as a stratified medium with no horizontal variations. The assumption of no horizontal variations is usually valid during periods of stable weather. Reference 1 reported concurrent soundings, 40 miles apart, as showing that "horizontal gradients are generally not of any significant magnitude." The data points used to define a sound speed distribution aloft could easily be fit to some analytical function **V(y)**, where **y** is height above the ground (AGL) or mean sea level (MSL). Nevertheless, treating the atmosphere as layers of linearly varying sound speeds allows for several conveniences. Reference 4 demonstrates that the solutions to the differential equation defining the ray paths in an atmosphere with a linear sound speed gradient are circular arcs. Gradients based on nonlinear functions **V(y)** must be solved by more cumbersome methods (e.g., Runge-Kutta or Simpson's rule) using incremental time-steps since only a few simple functions can be integrated analytically. Section 3.5 presents three nonlinear functions of **V(y)** that can be integrated exactly. Circular arcs can be handled with simple algebra, where the ray path terminus in a single atmospheric layer can be calculated with one equation. Intersections of circular ray paths with topography segments defining the ground are also easier to solve.

Since the atmospheric model is composed of multiple layers, determining the path of a given ray involves calculating its exit point through each layer in a cumulative manner. If a ray enters the bottom of some layer and exits the top, the horizontal distance, $\mathbf{X_h}$, covered by the circular arc can be treated trigonometrically as

$$\mathbf{X_h} = \mathbf{H_1} \cdot \cot\left[\frac{\theta_1}{2} + \frac{\theta_2}{2}\right] \tag{4}$$

where

$\mathbf{H_1}$ is the layer thickness;
θ_1 is the entrance angle of inclination;
θ_2 is the exit angle of inclination.

If the ray had turned within that layer, the horizontal range from entry point to turnover point is given as

$$\mathbf{X_h} = \frac{\mathbf{V_1} \cdot \mathbf{H_1}}{(\mathbf{V_2} - \mathbf{V_1})} \cdot \tan(\theta_1) \tag{5}$$

where

V_1 is the speed of sound at the bottom of the layer;
V_2 is the speed of sound at the top of the layer.

3.2 TOPOGRAPHY CONSIDERATIONS

In the flat topography model, the return point for the ray has a range ($\mathbf{X_T}$). This range can be obtained by simply doubling the sum of the distances calculated by Equations (4) and (5) in the passage through the different atmospheric layers:

$$\mathbf{X_T} = 2 \cdot \frac{\mathbf{V_{NTP}} \cdot \mathbf{H_{NTP}} \cdot \tan(\theta_{NTP})}{\left(\mathbf{V_{(NTP+1)}} - \mathbf{V_{NTP}}\right)} + 2 \cdot \sum_{i=0}^{NTP-1} \mathbf{H_N} \cdot \cot\left[\frac{\theta_i}{2} + \frac{\theta_{i+1}}{2}\right] \tag{6}$$

The subscript NTP refers to the layer where the ray turns downward. Since there are no horizontal variations in the defined atmospheric medium, each ray path is symmetrical about the vertical line passing through the turnover point. Ray intersections with a flat topography are simply the ranges of the rays. Rays touching down on water are defined as completely reflected. In the flat earth model, it is only necessary to multiply the distances to focal points on water until land is encountered, rather than calculate individual ray reflections. These shortcuts no longer apply when it becomes necessary to include a topography description of varying elevations. Without the flat-earth assumption, it is necessary to examine the ray path arc in each layer for an intersection with a topography segment. GZ may even be elevated above the surrounding terrain such that some rays turn more than once, causing a phenomenon called *ducting*. Ray reflections on water become asymmetrical when GZ is elevated, and each ray must be traced to its land terminus. The ray-topography intersection point is calculated algebraically by solving for the intersection between a line and circle. Many rays exit the scene of interest without touching down. When two real roots lie on the relevant part of the ray path arc, the one closer to GZ is taken as the intersection point.

Although time-of-travel for a ray traversing an atmospheric layer is easily calculable, such a quantity is not used in the current SIPS model. The arrival time for a ray undergoing skipping on water has been of interest because the number of skips required to reach a given point can be one or many, depending on the angle of departure. If the times of arrival steadily increase with the number of skips, then this fact would provide insight into the quality of the perceived sound across a large body of water. The complete derivation can be found in Reference 2. A relationship for the time $\mathbf{T}$ required for a ray to cross an atmospheric layer of thickness $\mathbf{H_1}$ with the same angles of entry and departure described for distance calculations is given:

$$\mathbf{T} = \frac{\mathbf{H_1} \cdot \cos(\theta_1)}{\mathbf{V_1} \cdot [\cos(\theta_1) - \cos(\theta_2)]}\left[\ln\{\sec(\theta_2) + \tan(\theta_2)\} - \ln\{\sec(\theta_1) + \tan(\theta_1)\}\right]. \tag{7}$$

In the layer where the ray turns, $\theta_2 = 0$ deg, the relation for the total time in the turning layer becomes

$$\mathbf{T} = \frac{2 \cdot \mathbf{H_{NTP}}}{(\mathbf{V_{NTP+1}} - \mathbf{V_{NTP}})} \cdot \ln[\sec(\theta_{NTP}) + \tan(\theta_{NTP})]. \tag{8}$$

A simple numerical case using the last equation was examined for a single-layer, positive-gradient atmosphere where the sound speed gradient was 0.05 per second and $\mathbf{V_o} = 1100$ fps. A horizontal distance of $\mathbf{X_h} = 10000$ ft was chosen for a point where angles of departure would be determined such that the rays would skip and touch down at $\mathbf{X_h}$ after zero, one, two, ..., 50 bounces. The results showed that the fastest arrival was for a ray that touched down without skipping ($\mathbf{T_o} = 9.0144122$ sec); a ray that skipped once showed $\mathbf{T_1} = 9.0714564$ sec of travel. The ray that skipped once traveled through the atmosphere where the sound speed was lower, hence the larger travel time compared to the no-bounce ray, which traveled higher in the layer. As the effects of more skips were calculated, the times increased, but began approaching an asymptote such that $\mathbf{T_{20}} = 9.0907134$ sec, and $\mathbf{T_{50}} = 9.0908778$ sec for 20 and 50 bounces, respectively. The times of arrival did not increase indefinitely with the number of ray skips on water.

Now that the basic elements have been cited, the details of implementing the theory into a functioning tool can be explored. The noise abatement problem is usually presented as explosive material of a given weight being detonated at a location surrounded by topography. This topography may include water and mountains and both noise-sensitive and nonsensitive areas. The procedure for defining the topography initiates at GZ as viewed from above on a map. A collection of radial lines define the surrounding topography as (x,y) points of distance from GZ and elevation. The elevation unit may be defined as either AGL or MSL. The MSL elevation is preferred since most topographic maps use this measure. The number and bearings of these radial lines depend on the locations of the sensitive areas. An increased number of radials are generated in the directions of the sensitive areas, while fewer are employed to define the nonsensitive areas.

Equations (2) through (6) assume two-dimensionality for ray tracing. Each topography radial defines a plane with GZ located toward the lower left corner. Sound rays emanate from GZ and propagate upward and to the right. Note that only a small portion of the total sound energy ever returns to earth, even in an atmosphere with severe inversions, because the sound speed deltas are small compared to the total sound speed. For example, if the sound speed on the ground is 1100 fps, and the highest value aloft is 1120 fps (high, but plausible), from Equation (3), $\theta_{MAX} = 10.8$ deg. The sound energy represented by rays leaving at angles greater than 10.8 deg does not return locally; the stratosphere eventually spreads and dissipates it. The ray-tracing process for a particular direction in SIPS begins by dividing θ_{MAX} into 100 initial angles of departure, such that the hemisphere of sound energy below θ_{MAX} is divided into bands of equal area. This technique allows for equal distribution of energy between rays. If the topography at GZ is not flat, there is a topographic slope angle θ_{TOPO} such that the difference is now $\theta_{MAX} - \theta_{TOPO}$. If $\theta_{TOPO} > \theta_{MAX}$, then no rays are sent out; but a quiet zone is not declared, since $\theta_{MAX} = 0$ is a requirement for a quiet zone. The detailed explanation for calculating the initial angles of departure is given in Reference 1, but the recursive relationship for generating them is given by:

$$\theta_i = \sin^{-1}\left[\frac{[\sin(\theta_{MAX}) - \sin(\theta_{TOPO})]}{100} + \sin(\theta_{i-1})\right] \tag{9}$$

The first angle of departure θ_1 is calculated from Equation (9) by letting $\theta_{i-1} = \theta_{TOPO}$. One hundred rays is an arbitrary choice, but this number has worked well. More rays can be sent out if more definition is needed in the output. As discussed earlier, different values of θ_{MAX} and θ_{TOPO} can exist for each azimuth of interest.

3.3 FOCAL POINT DEFINITION

For each initial angle of departure, a pair of rays is sent out. For example, if a ray with initial angle of departure θ_1 is sent out and calculated to have intersected with a topography segment at a range $\mathbf{R_1}$, a second ray is sent out at a slightly smaller angle:

$$\theta_1' = \theta_1 - (.001 \cdot \theta_1).$$

If this ray touches down at some range $\mathbf{R_1'}$, the difference, $\mathbf{R_1} - \mathbf{R_1'}$, is recorded and compared to that of the next pair, and so on, until a change of sign is noted. This change of sign indicates that the relative positions of the pair's touch-down points have switched. The switch means that between the two pairs there exists a point where a ray and its partner would have been coincident, mathematically indicating an acoustic focal point.

The heart of the SIPS algorithm for locating focal points is the change of ray pair positions, but not all such switches are due to true focusing structures in the atmosphere. Some focal points are artifacts produced by the technique of dividing the atmosphere into layers of linearly varying properties. Consider an atmosphere defined as two positive sound-speed gradient layers where the upper gradient is greater than the lower. Assume a flat terrain for simplicity, and calculate ray ranges as the initial angles-of-departure increase. A plot of hypothetical, ray range versus angle-of-departure is shown in Figure 7. The ray return range increases steadily with increasing departure angle until a ray enters the upper layer of greater positive gradient. At this point, a discontinuity in the range occurs and the range begins to decrease. Point 1 of Figure 7 is due to the discontinuity in the atmospheric properties and is not a true focal point. Point 2, however, is due to the greater refractive effects of the more positive gradient layer and is a true focal point with numerous ray returns at about the same range. A large concentration of ray returns indicates an increase in sound overpressure in that area. In addition, the SIPS focal point algorithm checks the $\mathbf{V_{TP}}$'s of the rays involved in the possible focusing condition. If the $\mathbf{V_{TP}}$ values bracket the sound speeds at any layer interface, the condition is known to be a false focal point caused by discontinuity in the atmospheric definition. False focal points are not entirely useless; however, including them among true focal points produces a more conservative prediction. False focal points indicate positive atmospheric sound speed gradients, which give rise to focusing if the layers are thick enough.

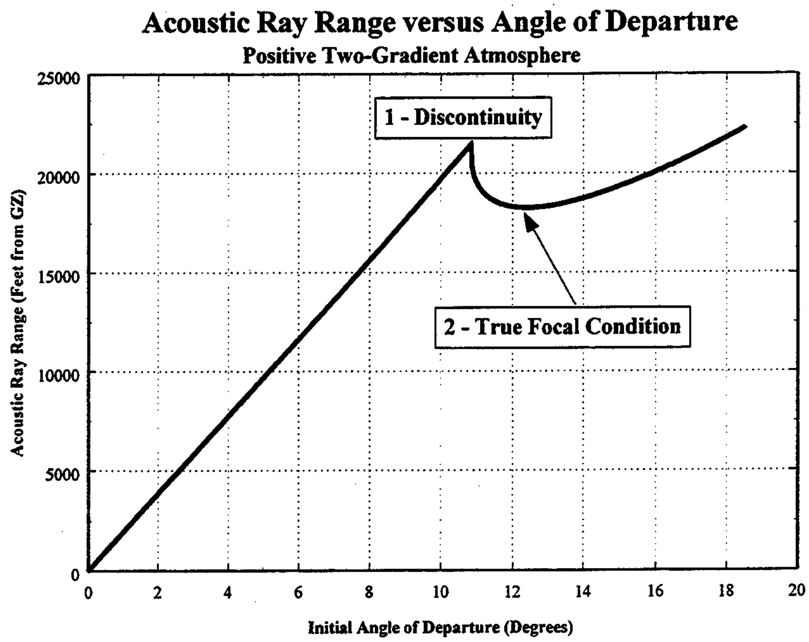

FIGURE 7. FLAT-EARTH ACOUSTIC-RAY RANGE VERSUS ANGLE-OF-DEPARTURE FOR A POSITIVE TWO-GRADIENT ATMOSPHERE

As modeled by SIPS, an acoustic focal point is a mathematical point where the sound energy can be imagined as infinite. Field measurements (References 7 through 11) have shown that the maximum overpressure increase above the expected level tends to be between 15 and 16 dB (a six-fold increase). A rare 20-dB (ten-fold) increase was reported from a shock tube experiment. Most increases, however, are less than 10 dB. The acoustic, ray-tracing technique used in SIPS represents the magnification of sound energy by the convergence of lines (acoustic rays) that are normal to the propagating sound wave surface. At some point, the air will limit the increase in overpressure and the sound energy will be spread over some finite area. SIPS records a focal point as 15 dB above the expected level.

An important condition to consider is ray returns to earth that do not satisfy the focusing definition. Reference 1 provides the means of calculating multiplication factors, which are applied to an average expected overpressure to show the increase in the sound energy concentration. The multiplication factor ($\mathbf{M_F}$) at some point is determined by comparing the pressure of sound undergoing spherical spreading ($\mathbf{P_1}$) to that in a refractive atmosphere ($\mathbf{P_2}$), so that

$$\mathbf{P_2 = P_1 \cdot M_F}.$$

In an atmosphere where spherical spreading occurs, acoustic rays diverge with distance from GZ. A refractive atmosphere with rays bending back toward the ground will generally have less distance between rays at the same range. Again, ray pairs sent out with a $\Delta\theta_o$ difference between the angles of departure can provide the ray divergence to be used in determining $\mathbf{M_F}$. Acoustic energy density is inversely proportional to the area between diverging rays. Since the rays are traveling in a plane, one factor of the area can be 1, so that the area becomes the distance between the rays at some range **R**. The distance between the spherically spreading ray pair at range **R** is $\mathbf{A_1} = \mathbf{R} \cdot \Delta\theta_o$. The distance between the rays in the downward refractive atmosphere when they touch down is $\mathbf{A_2} = \Delta\mathbf{R} \cdot \mathbf{sin}(\theta_o)$. The energy is also proportional to the square of the pressure; thus, a relation between the pressures, areas, and $\mathbf{M_F}$ is available:

$$P_2 = P_1\left[\frac{A_1}{A_2}\right]^{1/2} = P_1 \cdot M_F = P1\left[\frac{R}{(\Delta R / \Delta\theta_o)\sin(\theta_o)}\right]^{1/2} \tag{10}$$

Reference 1 makes no mention of calculating $\mathbf{M_F}$ for quiet zones. If the same logic is applied to determine a pressure reduction in a negative gradient atmosphere, it is found that even at $\theta_o = 0$, the ray path curves upward, never to return. Therefore, theoretically, no rays or sound should be detected at the ground. Ray tracing techniques offer no tools for calculating pressure reductions; yet, there is the intuition that some quiet zones are quieter than others. The problem with quantifying quiet zones experimentally is that frequently the noise level falls below ambient so that either instrumentation cannot record it or the reading cannot be trusted. Reference 7 lists 10 field measurements compared with predictions and indicates a reduction of 30 dB for one quiet zone, and a reduction of 20 dB for four other quiet zones. SIPS currently treats all quiet zones equally and does not attempt to predict sound levels.

3.4 AVAILABLE BLAST PROPAGATION MODELS

The predicted sound pressure levels must be compared to a standard if there is to be any way of predicting intensification due to refraction. Reference 4 presents a log-log plot based on overpressure measurement versus distance for various explosive charge weights detonated on the surface. Reference 7 presents an empirical relationship for this data that it calls the "expected surface air-blast pressure from an explosion with no atmospheric refraction of the blast wave." In SIPS, the background standard is called an "average expected overpressure." This background average is based on experimental data, which by nature must reflect the effects of quiet zones, focal points, and other conditions, rather than an unrealistic nonrefracting atmosphere. The expression from Reference 4 utilized in SIPS for the average expected overpressure expressed in pounds per square inch is:

$$P = 226.62 \cdot \left[\frac{W^{1/3}}{R}\right]^{1.407} \tag{11}$$

where **W** is the TNT-equivalent charge weight in pounds, and **R** is the range in feet from the explosive. Reference 12 identifies this functional form as Hopkinson scaling for invariant ambient conditions; the more general form (Sach's scaling) is also a function of ambient atmospheric pressure. Given **P**, the sound pressure level (**SPL**) expressed in decibels is given by

$$\mathbf{SPL(dB)} = 10 \cdot \log_{10}\left[\frac{\mathbf{P}}{\mathbf{P_o}}\right]^2; \mathbf{P_o} = 2.9 \times 10^{-9}\,\mathbf{psi} \tag{12}$$

$\mathbf{P_o}$ is the zero-decibel reference pressure to which overpressures are compared. Upon substitution of Equation (11) into Equation (12), the final relationship as employed in SIPS becomes:

$$\mathbf{SPL(dB)} = 20 \cdot \log_{10}\left[\frac{226.62 \cdot \mathbf{W}^{.47}}{\mathbf{R}^{1.41}}\right] + 170.75 \tag{13}$$

There are several experimental based blast curves identified by their exponential rate of decay of sound overpressure with distance. A comparison of the various models is given in Reference 12, in which Equation (13) is called the "BRL model." All models based on experimental data decay faster than predicted by spherical spreading.

3.5 EXACT ANALYTICAL FUNCTIONS

As a final matter of interest, several atmospheric models are presented with sound speeds $\mathbf{V(y)}$ that increase with altitude and are functionalized as (1) linear, (2) exponential, and (3) hyperbolic cosine profiles. These functions can be analytically treated such that the total ray range $\mathbf{X_T}$ in a flat-earth model can be given as a function of departure angle θ_o only. Atmospheres with these sound speed distributions are not implausible and shed light on the focusing condition $\frac{\mathbf{dX_T}}{\mathbf{d\theta_o}} = 0$. Only Snell's law,

$$\frac{\cos(\theta_o)}{\mathbf{V_o}} = \frac{\cos(\theta(\mathbf{y}))}{\mathbf{V(y)}} = \delta, \text{ and } \frac{\mathbf{dy}}{\mathbf{dx}} = \tan(\theta)$$

are needed. Since $\cos(\theta) = \delta\mathbf{V}$, in general

$$\mathbf{X_T} = 2\int_{\theta_o}^{0} \frac{\cos(\theta)}{\sin(\theta)}\mathbf{dy} = 2\int_{\mathbf{V_o}}^{\mathbf{V_{TP}}} \frac{\delta\mathbf{V}}{\sqrt{1-(\delta\mathbf{V})^2}}\mathbf{dy}.$$

Either integral type can be used, depending on which type is more easily integrated as y is a function of θ. In the three cases below, the θ integral is easier.

3.5.1 Linear Profile

$$\mathbf{V(y)} = \mathbf{V_o} + \mathbf{Ky} \text{ where } \mathbf{K} > 0$$

where

K = sound speed gradient.

An illustration of a positive linear sound speed profile is shown in Figure 3. Given that

$$\cos(\theta) = \delta\mathbf{V} = \delta\mathbf{V_o} + \delta\mathbf{Ky} \longrightarrow \mathbf{dy} = \frac{-\sin(\theta)\mathbf{d}\theta}{\delta\mathbf{K}}, \text{ then}$$

$$\mathbf{X_T} = \frac{2}{\delta\mathbf{K}}\int_{\theta_o}^{0} -\cos(\theta)\mathbf{d}\theta = \frac{2\mathbf{V_o}}{\mathbf{K}}\tan(\theta_o).$$

This atmospheric profile, by itself, does not give rise to focusing conditions because $\frac{\mathbf{dX_T}}{\mathbf{d}\theta_o} = 0$ does not occur, but the sound intensity on the ground is greater than that expected by spherical spreading.

3.5.2 Exponential Profile

$$\mathbf{V(y)} = \mathbf{V_o} \cdot \mathbf{e}^{(\mathbf{h}\cdot\mathbf{y})}.$$

See Figure 8. The constant **h** is used for scaling. Beginning with

$$\cos(\theta) = \delta \cdot \mathbf{V_o} \cdot \mathbf{e}^{(\mathbf{hy})},$$

the next relationship is

$$\ln(\cos(\theta)) - \ln(\delta\mathbf{Vo}) = \mathbf{hy} \longrightarrow \mathbf{dy} = -\frac{1}{\mathbf{h}}\frac{\sin(\theta)}{\cos(\theta)}\mathbf{d}\theta.$$

This function simplifies the integral to give

$$\mathbf{X_T} = -\frac{2}{\mathbf{h}}\int_{\theta_o}^{0}\mathbf{d}\theta = \frac{2\theta_o}{\mathbf{h}}. \quad \frac{\mathbf{dX_T}}{\mathbf{d}\theta_o} = \frac{2}{\mathbf{h}},$$

a constant greater than zero, showing that the range $\mathbf{X_T}$ is proportional to θ_o. This profile also intensifies sound levels on the ground, but does not cause focusing.

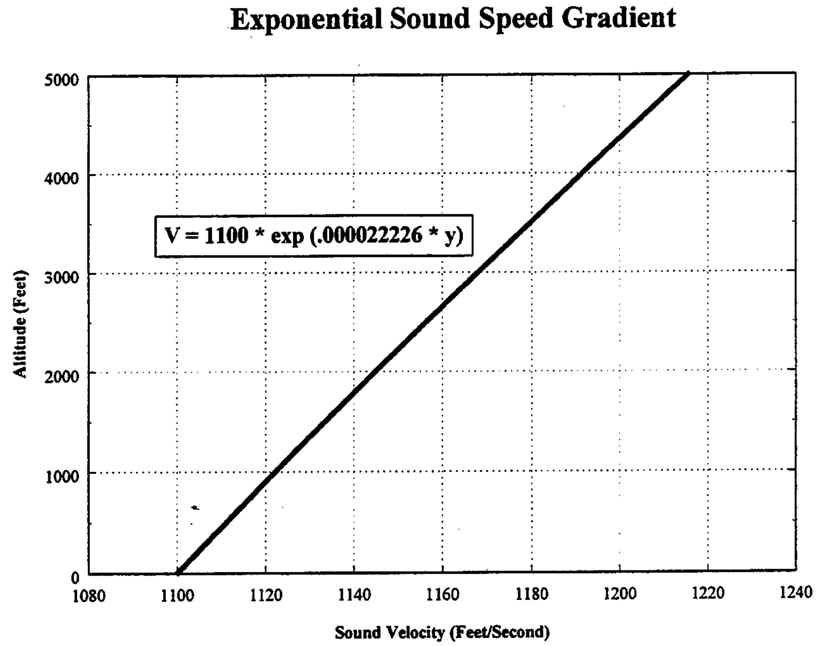

FIGURE 8. EXPONENTIAL SOUND SPEED GRADIENT

3.5.3 Hyperbolic Cosine Profile

$$\mathbf{V(y)} = \mathbf{V_o \cosh (hy)}.$$

See Figure 9. To relate **y** and θ, the same form,

$$\cos(\theta) = \delta \mathbf{V_o \cosh (hy)},$$

can be used to provide

$$\frac{\cosh^{-1}}{\mathbf{h}}\left[\frac{\cos(\theta)}{\delta \mathbf{V_o}}\right] = \mathbf{y} \longrightarrow \mathbf{dy} = \frac{-\sin(\theta)\mathbf{d}\theta}{\mathbf{h}\sqrt{\cos^2(\theta) - (\delta \mathbf{V_o})^2}}.$$

The integral becomes

$$\mathbf{X_T} = \frac{-2}{\mathbf{h}\sqrt{1-(\delta \mathbf{V_o})^2}} \int_{\theta_o}^{0} \frac{\cos(\theta)\mathbf{d}\theta}{\sqrt{1 - \frac{\sin^2(\theta)}{1-(\delta \mathbf{V_o})^2}}} = \frac{\pi}{\mathbf{h}}.$$

The hyperbolic cosine profile behaves as a lens to focus all sound leaving GZ to a point $\pi/\mathbf{h}$ regardless of the angle of departure, since $\frac{\mathbf{dX_T}}{\mathbf{d\theta_o}} = 0$ for all θ_o.

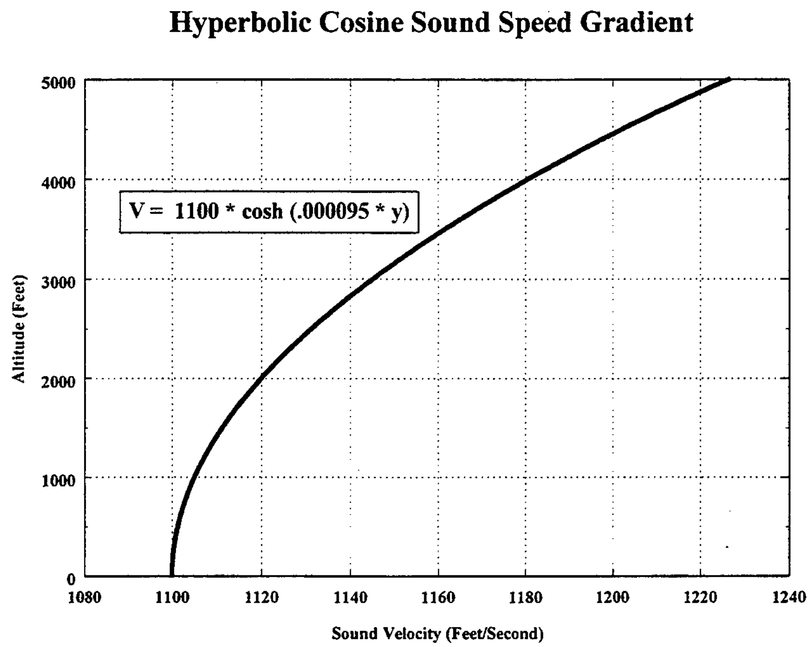

FIGURE 9. HYPERBOLIC COSINE SOUND SPEED GRADIENT

4.0 SIPS PROGRAM HISTORY

SIPS was developed in the early 1970s by Dr. N. H. Gholson. He employed the ray-trace theory documented in Reference 4. The program is written in the FORTRAN programming language and originally required a large mainframe computer to run. The increase in computing power over the years now makes it possible to execute SIPS on a personal computer. Initially, topography of the area of interest was not included in the program, yielding a flat-earth model. This flat-earth model has not been a shortcoming at NSWCDD because of the limited topographic features. The Potomac River, which constitutes the firing range, is the only outstanding topographical feature. The river has always been annotated in a terrain file so that sound ray skipping on water could be calculated.

In May 1975 the noise abatement program became a requirement before every explosive operation at NSWCDD. The number of complaints decreased to three or four per year. A hypothesis for this drop held that there were either thermal inversions or wind shears during the early morning or late evening hours. SIPS predicted sound focusing for this type of weather event. As a result, explosive operations began to be scheduled for the middle of the day to avoid the unfavorable conditions existing during the morning and evening hours.

Soon after SIPS was put into use at NSWCDD, the program's output was changed to represent a map for easier interpretation. The original program produced numerous pages of printed output cataloging the ranges of the traced rays for each azimuth. A magnification of 20 dB was added to the average expected overpressure when a focusing condition was predicted.

A later revision reduced this magnification to the present, 15-dB value because experimental data showed this as more realistic. If a quiet zone was predicted, the average expected overpressure value was reported because NSWCDD wanted to remain conservative. Presently, SIPS output reports that the sound would be less than the average expected in a quiet zone, but no number is reported.

The Naval Science Assistance Program (NSAP) contacted NSWCDD in 1976 to assist the Commander of the Third Fleet (COMTHIRDFLT) with noise complaints from Maui in Hawaii. Residents objected to noise from the Armed Services firing range on the nearby island of Kahoolawe. SIPS was examined as a possible noise abatement tool with its implementation being called for as soon as possible. The flat-earth model in use at NSWCDD conveniently allowed many mathematical shortcuts to reduce computing time. A more general version of SIPS had to be created for Kahoolawe so that topography around GZ locations could be included. Meteorological data was the more difficult issue: measurements from Lihue on Kauai and Hilo were woven together to provide an atmospheric profile for use over Kahoolawe. The meteorological data was wired to the Fleet Numeric Weather Central in Monterey, California, where the SIPS program was executed. The output was returned to a line printer at Fleet Weather Center in Pearl Harbor where a decision was made for exercises on Kahoolawe, as described in Reference 13. Improvement with regard to complaints was not as clear as at NSWCDD, but the procedure was carried out until the closing of the Kahoolawe test range.

Lawrence Livermore National Laboratory (LLNL) requested and received the SIPS code in the summer of 1990, as acknowledged in Reference 14, for use at their Site 300 test area. The test site is approximately 1300 ft MSL, while the residential area of concern lies 6 miles east at an elevation of 100 ft MSL. A series of hills (approximately 1500 ft high) surrounds the site, so that uneven hilly terrain lies between the site and residential area. Because of such uneven terrain and the difference in elevation, different local weather conditions may occur to modify the ray-propagation behavior following detonation. Concern for discrepancies between test data and the predictions prompted LLNL to modify the SIPS code. This modification involved adding an algorithm to account for different weather conditions downstream of GZ. The modified code was renamed "Livermore Atmospheric Propagation" (LAP), but otherwise adopted the entire logic of SIPS. Reference 14 documents the effort of LLNL. Operationally, LAP was not implemented, and LLNL employs the SIPS and BLASTO (blast overpressure, Reference 15) codes because logistics for multiple meteorological stations became excessive.

Beginning in 1991, SIPS enhancements were made to account for the directivity of naval guns. Reference 6 reports that a difference of 14 dB is possible between peak sound levels in the far-field at the same distance in front and behind the gun. The first directivity change to the NSWCDD SIPS was for the 16-inch/50 naval gun. SIPS treated the gun blast as an open-air spherical charge and routinely overpredicted excessive noise levels behind the gun. Gun tests were needlessly canceled when high overpressures were inappropriately predicted in sensitive areas behind the gun. Subsequent changes included the directionality blast curves for the 5-inch/54, and 8-inch/55 naval guns, Reference 8.

A major improvement was also made to the meteorological data collection system at NSWCDD in 1991. A capability for more data samplings resulted in a much more detailed description of the atmosphere. Instead of temperature-wind data being sampled every few hundred feet, an order-of-magnitude improvement in resolution became available. This new situation immediately created an unanticipated problem for SIPS. The boundary layer near the ground appeared as a severe wind shear and had a very large impact on the SIPS predictions. SIPS began to predict focal areas several miles around NSWCDD, some of which caused program postponements. The gun directivity changes eased some of the severe predictions, but the boundary layer had always existed and was now causing problems because it could now be recorded and input to SIPS. The more variable properties of the boundary layer were a function of the surrounding buildings at the meteorological ground station and probably did not apply over the water and surrounding land. A minor change to the SIPS code negated the effects of the first atmospheric layer so that the refraction began at a slightly higher level. The focal areas that occur farther downrange are due to more stable atmospheric structures at much greater altitudes. Focusing predicted within one mile of GZ is not of interest since the noise is inside NSWCDD.

On 3 November 1993, Hill Air Force Base of Ogden Utah destroyed by open detonation two C-3 Poseidon second-stage rocket motors at UTTR. The resulting complaints from Salt Lake City prompted the Strategic Systems Program Office to contact NSWCDD about SIPS. Beginning in September 1994, SIPS—along with two other sound propagation programs—was employed before every disposal operation. As of this writing, there have been approximately 120 operations with only one complaint. In order to perform at this reliability level, SIPS has been modified to improve the user interface and interpretation of predictions. The following section details these modifications and discusses plans for future revisions.

5.0 UTTR SIPS MODIFICATIONS

The 3 November 1993 detonation at UTTR prompted many complaints along the Wasatch Front. The state of Utah suspended all Poseidon C-3 second-stage operations until a plan of action to handle the noise was approved. When operations resumed, September 1994, they were on a demonstration basis only. The state of Utah required that five localities be monitored for noise levels during disposal operations and that noise prediction models be run. The focus of this effort was to prevent the disruption of the population centers of the Wasatch Front. The UTTR, on the western bank of the Great Salt Lake, lies within 60 to 100 kilometers of these population centers, as shown in Figure 10.

To describe the topography of the region, radial lines were extended outward from GZ with the most populated region, North Ogden to Riverton, falling within the angular segment between 75 and 130 deg off true north. This angular segment was divided into 2.5-deg intervals to adequately define the region. A second region, from Riverton to Grantsville, was divided into 5-deg intervals. The remainder of the area around UTTR, (160 to 360 deg and 0 to 70 deg) was divided into 10-deg intervals.

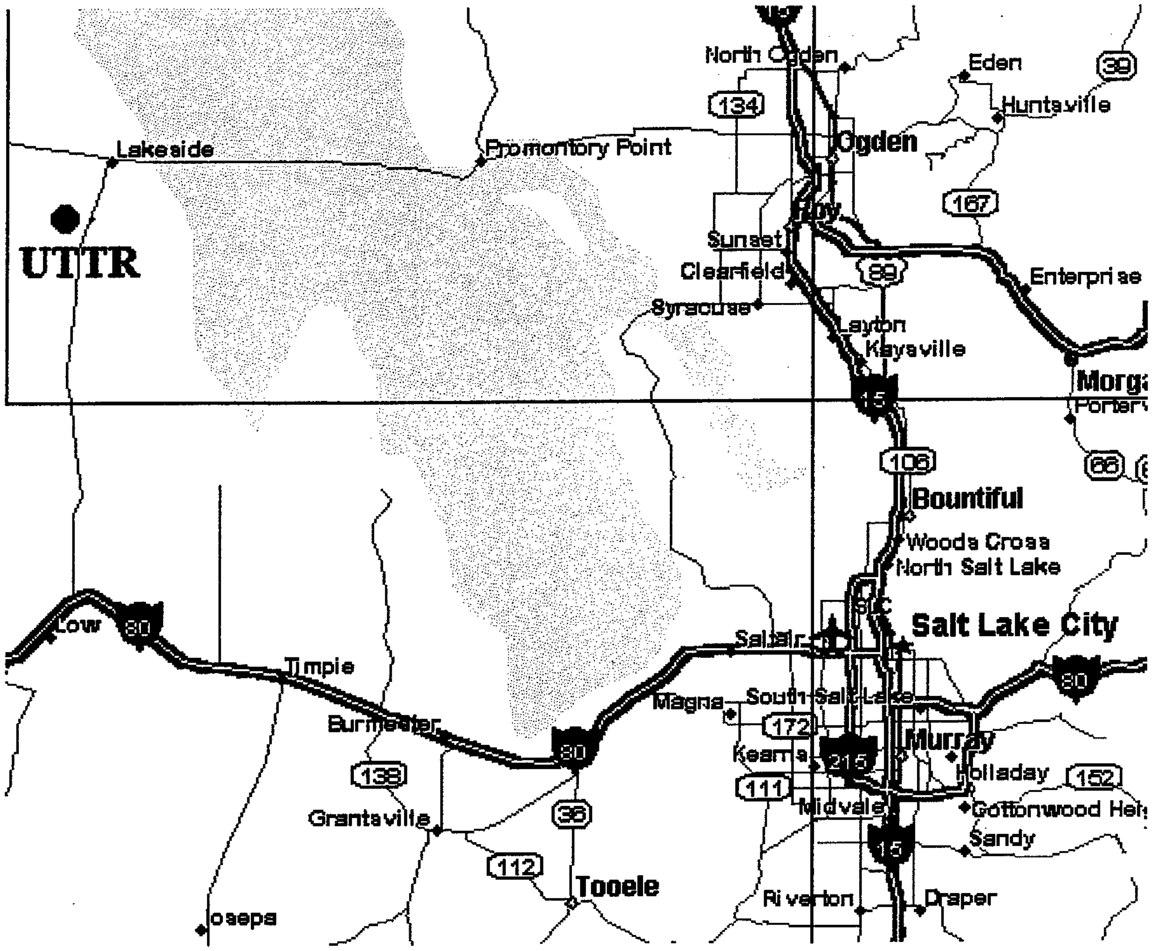

FIGURE 10. POTENTIAL AREA OF NOISE IMPACT FOR THE UTAH TEST AND TRAINING RANGE

Originally, the SIPS output map was overlaid with a grid to match a large wall-mounted topography map of the area. The line-printer map type of output is difficult to interpret at best. Mistakes can be made if the person responsible for making the "GO" or "NO GO" decision is not experienced in the interpretation of the output. Therefore, the output map was completely redone. In an iterative process, aided by UTTR personnel, the output map became graphical, with the inclusion of a topographic map locating the populated areas. Additionally, the graphical output map indicates ("+" symbol) the locations of ray returns that do not satisfy the focal criteria. A comparison of this advancement is shown in Figures 11 and 12 for the same meteorological data.

Also developed for UTTR were two other improvements to the understanding of SIPS and sound propagation, sound velocity profile, and ray-trace drawings. The sound-velocity-profile plot is an overlay of the profiles for the five, state-mandated directions. The ray-trace drawings are meant to show the cause and effect relationship between the sound velocity profile and the propagation path. With this set of plots, the user can get a better understanding of why the output map looks the way it does.

M A P   K E Y

BALLOON 6037 4/29/96 1455Z

OVERPRESSURE IN PASCALS AND IN DECIBELS (PARENTHESES)
FOR THE FOLLOWING TNT EQUIVALENT CHARGE WEIGHTS.

FOCAL POINTS	20000.0 LBS.	40000.0 LBS.	60000.0 LBS.	80000.0 LBS.
(A)	123.5 Pa (136 dB)	171.6 Pa (139 dB)	208.0 Pa (140 dB)	238.4 Pa (142 dB)
(B)	69.5 Pa (131 dB)	96.5 Pa (134 dB)	116.9 Pa (135 dB)	134.0 Pa (137 dB)
(C)	39.1 Pa (126 dB)	54.3 Pa (129 dB)	65.8 Pa (130 dB)	75.4 Pa (132 dB)
(D)	22.0 Pa (121 dB)	30.5 Pa (124 dB)	37.0 Pa (125 dB)	42.4 Pa (127 dB)

```
Q   I N D I C A T E S   A   Q U I E T   S E C T O R
RESULTS VALID FOR TOPOGRAPHY OF UTTR TTU TEST AREA LAKE EL 4212 FT.
( 41.75N, 113.00W) UPPER LEFT CORNER
+-------------+-------------+-------------+-------------+-------------+
.             .             .             .             .       |     .
.             .             .             .             .       |     .
.             .             .             .             .       |     .
.             .             .             .             .       |     .
.             .             .             .             .       |     .
.             .             .             .             .       |     .
.             .             .             .             .       |     .
.             .             .             .             .       |     .
.             .             .             .             .       |     .
.             .             .             .             .       |     .
+-------------+-------------+-------------+-------------+-------------+
.             .             .             .             .       |     .
.             .             .             .             .       |     .
. Q  Q  Q     .             .             .             .       |     .
.           Q .             .             .             .       |     .
.             .             .             .             .       |     .
.             .             .             .             .       |     .
.             .             .             .             .       |     .
.             .             .             .             .       |     .
.             .             .             .             .       |     .
.             .             .             .             .       |     .
+-------------+-------------+-------------+-------------+-------------+
.             .             .             .             .       |     .
.             .             .             .             .       |     .
.             .             .             .             .       1     .
.             .             .             .             .       |     .
.    X        .             .             .             .       |     .
.             .             .             .             .       |     .
.             .             .             .      2      .       |     .
.             .             .             .             .       |     .
.             .             .             .             .       |     .
.             .             .             .             .       |     .
+-------------+-------------+-------------+-------------+----D-3------+
.             .             .             .             .       |     .
.             .             .             .             .       | D   .
.       A     .             .             .             .       |     .
.          A  .             .             .             .       |     .
.             .             .             .             .       4     .
.    A        .             .             .             .      5|     .
.             .             .             .             .       |     .
.             .             .             .             .       |     .
.             .             .             .             .       |     .
.             .             .             .            D.       |     .
+-------------+-------------+-------------+-------------+-------------+
.             .             .             .             .      D|     .
.             .             .             .             .       |     .
.             .             .             .  D          .       |     .
.             .             .             .           D .       |     .
._____________._____________._____________.__________D__.D_____D______.
```

FIGURE 11. SIPS TEXT OUTPUT FOR UTTR BALLOON 6037

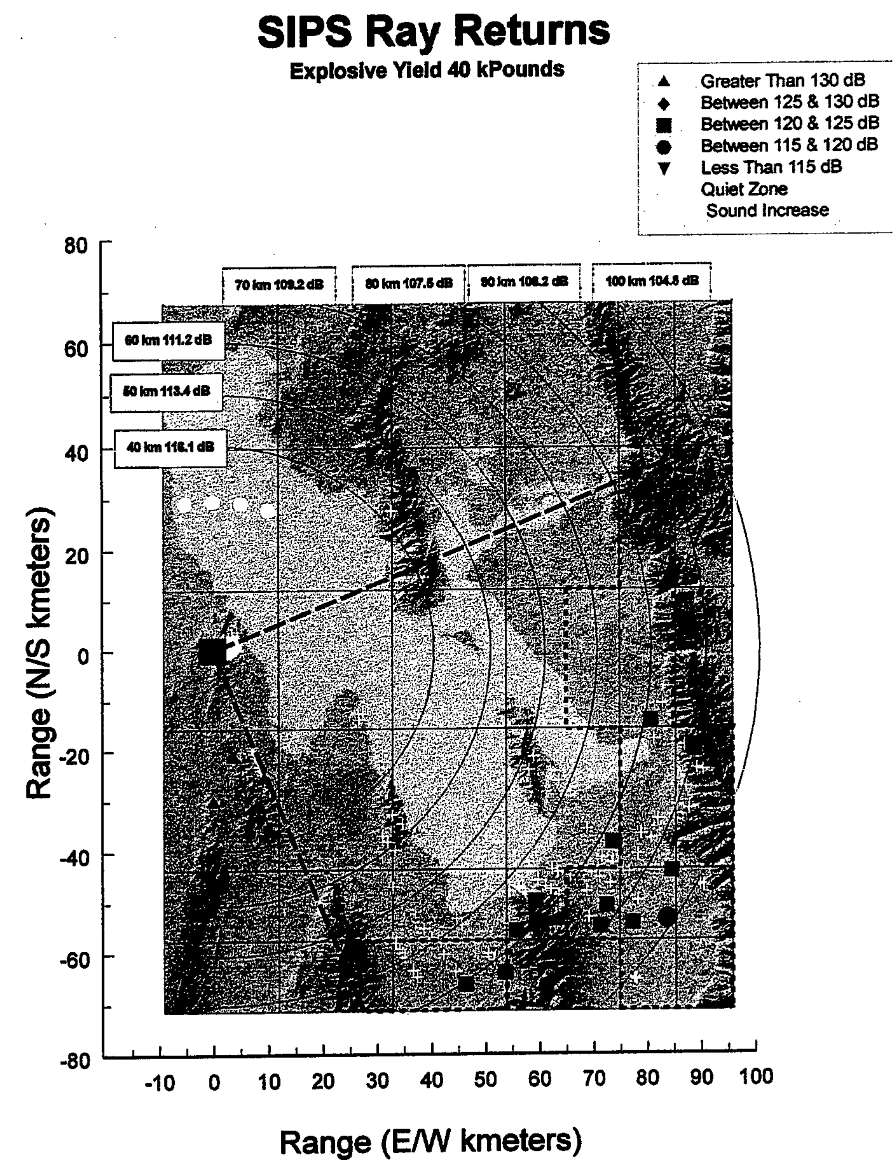

BALLOON 6037 4/29/96 1455Z

FIGURE 12. SIPS GRAPHICAL OUTPUT FOR UTTR BALLOON 6037

5.1 FUTURE MODIFICATIONS

The above modifications to SIPS will not be the last; development will continue to improve both the accuracy and output interpretation. The first modification will be electronic generation of the topography file. Presently, the radial lines for the file are generated by placing a protractor and scale on a United States Geological Survey (USGS) topography map and reading the elevation at different distances. This method is a tedious process where the potential for error is rather high. A more accurate and faster way to generate the topography file is to use unclassified digital elevation data from the National Imagery and Mapping Agency, Reference 16.

A second modification to improve ease of use will be a new user interface. This will allow the user to input all requested information at the outset, at which point the program executes unimpeded. Finally, as mentioned earlier, three-dimensional effects are being examined in an effort to improve prediction accuracy. This approach should also allow for the simulation of nonhorizontal surface reflections to account for echoing.

6.0 SIPS PROGRAM VALIDATION

The first efforts to validate SIPS were made in 1974 at NSWCDD and documented in Reference 6. A procedure was established to compare SIPS predictions with measured sound levels. A weather balloon was initially launched and areas of predicted sound focusing and quiet zones were established. Personnel equipped with sound level meters went to these areas and waited to record the explosive event. The meters were set to record the peak sound level on the flat scale as directed for impulse noise. Sound meter readings were collected and compared to predictions from weather balloon data taken during the time of the explosive event. The average expected sound level for a given distance was determined, by means of the guidelines of Reference 4, based on numerous charge weights and distances. The data table of 11 events shows a maximum increase of 15 dB at a focal region and a maximum reduction of 30 dB in a quiet zone. The uncertainty with Reference 7, however, is that the meteorological data employed for the predictions and sound-level measurement locations went unreported.

An ambitious attempt at validation was made in the summer of 1978 on the island of Maui. Instrumentation consisted of sound level meters and a state-of-the-art portable meteorological data collection system. The SIPS computer code was executed on the mainframe computer at NSWCDD. Meteorological data from Maui was read over the telephone and punched on cards for input. SIPS predictions were then telephoned back as intensities with locations representing a grid-map of the western side of Maui. Observers were sent to the prediction sites, when possible, and awaited the detonation of small high explosive (HE) charges on Kahoolawe. After ten days of measurements, the relationship between SIPS predictions and the sound measurements was not clear.

Several difficulties were immediately apparent during the Maui validation tests. As identical HE charges were set off on Kahoolawe at 5-minute intervals, the peak sound levels on

Maui varied over a wide range in a period of minutes. Air turbulence was seen as a major factor in the variation. Most of the sound measurements were made on or near the slopes of Mt. Haleakala, which has an elevation of 10,023 ft above sea level. Large downdrafts of cold air descended the mountain each morning; this caused the meteorological balloon to depart horizontally when launched from the beach. Additionally, it was reasoned that the upper air winds were drastically affected by the presence of the mountain, further upsetting the assumption of constant horizontal atmospheric properties. The main difficulty during this validation test was the availability of the LORAN-C signals for the calculation of wind information. In this remote location, signals were quite weak, only strengthening to usable levels between late evening and early morning hours. And finally, meteorological data should be collected as near GZ as possible; on the island of Kahoolawe, collection near GZ was not possible and could have been dangerous.

The issue of air turbulence affecting sound levels prompted a review of July 1978 gun blast test data (Reference 8) collected at the Naval Air Warfare Center, China Lake, California. A 5-inch/54-caliber naval gun was mounted in the desert and repeatedly fired while meters at fixed locations recorded peak sound levels. Meteorological data was collected near the site at a two-hour interval during the firings. SIPS was run after-the-fact for the sound meter locations. Because of continuity between the serial meteorological data sets, the meteorological data was interpolated to match the gun blast time. In spite of the measures taken, sound intensity predictions and measurements rarely matched. The expectation to accurately predict a sound intensity at some specific location appeared to be excessively optimistic as the effects of even slight air turbulence came to be appreciated.

The validation of NSWCDD SIPS in Reference 7 was never a rigorous engineering validation by comparing predictions to measurements. Those tests were more oriented to finding how much overpressure magnification or reduction could be expected from focal points and quiet zones. In 1994 an opportunity to test SIPS in a more rigorous manner arose with the testing of a 155-millimeter/40-caliber towed howitzer at NSWCDD. Projectiles were fired through a low cloud layer to test a fuze malfunction. The weather conditions required for the tests allowed many focal areas to be predicted and measured. The firings occurred on three occasions in March 1994 during days of winds, rain, and overcast. Focal areas were produced in abundance and were consistent with the winds in their distribution. SIPS predictions did not consistently match measurements except in a general way.

The work since September 1994 at UTTR has generated a significant number of SIPS predictions and measured sound levels. A compact disc (CD) was published to document each scheduled operation of the 1995 and 1996 operating seasons (Reference 17). The Air Force weather office of Hill Air Force Base has recorded sound levels at the entrance to Antelope Island since the first season. This measurement provides a consistent reference point 65 kilometers from GZ. Additionally, the firm of Dames and Moore was hired to make sound measurements at various locations along the Wasatch Front between July 1996 and June 1997. A report, Reference 18, was released documenting this effort and included independent recommendations for program improvement. A thorough comparison of the predictions versus measurements will be undertaken shortly and a report will be published separately.

7.0 COMPLAINT MANAGEMENT

Currently no regulated guidelines or criteria exist for assessing annoyance related to a single noise event. Reference 19 stated that annoyance from a single noise event depends both on characteristics of the noise itself and on the community's perception of the noise. Characteristics of the noise include:

- The intensity of the noise;
- Its spectral characteristics;
- Duration of the sound;
- The number of repetitions;
- The abruptness of onset or cessation;
- Background noise when a particular noise event occurs.

Social surveys have found that community perception factors can include:

- The degree of interference of the noise with activity;
- Previous experience of the community with the particular noise;
- The time of day that the intruding noise occurs;
- Fear of personal danger associated with the activities of the noise sources;
- Socioeconomic status and education level of the community;
- The extent the people believe that the noise output could be controlled.

7.1 OPERATIONAL GUIDELINES

The only operational guidelines available are based on over 10 years of complaint logging in the NSWCDD area. During this proceeding, efforts were made to understand what generated each complaint. In the NSWCDD area, the level at which people began to complain occurred when the peak sound level exceeded 120 dB. Using this information, Dr. L. L. Pater developed a noise limit criterion, Reference 2, for NSWCDD. These guidelines represent the best compromise between cost, efficiency of range operations, and good community relations. The levels set forth in the criteria have stood well although the basic makeup of the community has changed. A larger percentage of the population no longer has financial ties to NSWCDD.

The criterion does not always work, however. The residents of Maui, during the summer of the 1978 SIPS validation, did not seem to be disturbed by a particular noise level. Complaints were registered when sound level measurements ranged from inaudible to 90 dB. It was hypothesized that residents may not have always been responding to sound; smoke from Kahoolawe clearly indicated when operations were underway. There was also a strong local movement to end military bombardment of Kahoolawe as it was traditionally purported to be a holy place.

The NSWCDD guidelines have also been used for evaluating the complaint potential for disposal operations at UTTR. The state of Utah imposed a noise limit of 130 dB peak on the flat scale, which by the criteria is the break point between a moderate and high risk of noise complaints. An operational noise limit of 120 dB was initiated, which for the distances involved, precludes sound focusing in populated areas. This limit has worked well in that there has been only one complaint registered since September 1994. That complaint came in May 1996 because of output misinterpretation. This also occurred before all of the graphical output modifications had been completed.

7.2 SIPS OUTPUT INTERPRETATION

Given that the meteorological data defining the atmosphere is a single sounding, some limitations had to be imposed on the use of SIPS and the interpretation of its output. The idea of predicting the exact locations of individual focal points has been dropped in favor of looking at areas or bands of focusing on the output map. Figure 12 shows circular swaths of focal point and ray return predictions that indicate concentrations over a large area. There is a tendency in the early use of SIPS to look at a sensitive area and approve an explosive operation if the predicted focal point was near, but not on, the area. Examining more azimuth directions around GZ and applying a connect-the-dot approach with the calculated focal points is seen as better than looking for direct hits on complaint-prone localities by individual focal points. Furthermore, any wind turbulence causes the focal areas to shift locations, disappear, and reappear within minutes, or sometimes seconds, as indicated by observations in Maui. Looking at areas, rather than points, partially compensates for the unpredictable short-term wind irregularities.

SIPS can predict areas of quiet with more accuracy than areas of sound magnification. Quiet zones are sectors rather than points with a simple calculation determining if all the sound energy is going to the stratosphere. If the speed of sound on the ground in a given direction is greater than that at any point aloft, sound traveling in that direction will curve upward without returning. Noise reductions can vary from slightly less than expected to inaudible above the ambient noise. Upper air variations will not affect the quiet zone prediction, as the maximum sound speed occurs at the ground.

8.0 CONCLUSION

All computer models that make predictions about sound distribution during an explosive operation will have some limitation based on the freshness of the weather data, how fast the weather is changing, or mathematical modeling assumptions. The purpose of these predictive models is to allow a user to make a "GO" or "NO GO" decision about an explosive operation based on where the model predicts the sound will go. If the model is too conservative, then no operations can be carried out. Too lax a model will open the user to noise complaints. The gray area between these two extremes is where the different models compete. Most are approximately equivalent in their predictive power with different methods of getting results and displaying the output. The user must become familiar with the particular model being used, compare predictions with any data that can be gathered, and keep good records of complaints so that experience can be gained for application to the "gray areas."

This report documents the theory behind SIPS as well as the evolutionary process the program has gone through to get to this point. Originally, personnel involved with SIPS felt that the exact location and amplitude of focal points could be determined. Using a point-by-point evaluation process between the SIPS predictions and actual measurements, this belief cannot be substantiated except in general terms. This does not mean that the program has not served a need. The manner in which SIPS has been implemented is in terms of a noise-complaint management tool. SIPS provides information on the areas that can expect both increased and decreased noise levels. In this manner, the user can determine the noise levels in a sensitive area where complaints are possible. Predictions of quiet zones covering those areas indicate an excellent time for explosive events.

Although most models make use of ray tracing, the technique is not universally accepted as the proper way to predict sound propagation in the atmosphere. Some think ray tracing alone can be too sensitive to small changes in the atmosphere and is not conservative enough. To enhance the quality of SIPS predictions, operations should be scheduled only on days when the weather is stable, not when a weather front is pushing through (Reference 4). Predictions made during unstable weather may not apply to the sensitive areas where different conditions may exist. In addition, predictions of focusing should be considered as areas rather than points since there is a tendency for them to drift. SIPS employs ray tracing because it is based on a simple mechanism that allows for a maximum exploitation of the weather data. It also lends itself to easy experimentation that can be graphically displayed; the last feature aids the user in acquiring experience with the model.

9.0 REFERENCES

1. Gholson, Norman H., *An Analysis Of Sound Ray Focusing,* NWL Technical Report TR-2834, Jan 1973, NSWCDD, Dahlgren, VA.

2. Pater, L. L., *Noise Abatement Program For Explosive Operations At NSWC/DL,* A paper presented at the Seventeenth Explosives Safety Seminar of the DDESB at Denver, CO, Sep 1976.

3. *U.S. Standard Atmosphere, 1976*, Environmental Science Services Administration, National Aeronautics and Space Administration, United States Air Force.

4. Perkins, Beauregard Jr. et al., *Forecasting The Focus Of Air Blasts Due To Meteorological Conditions In The Lower Atmosphere,* Report No. 1118 Oct 1960, Ballistic Research Laboratories, Aberdeen Proving Ground, NCD.

5. Thompson, R. J., "Ray Theory for an Inhomogeneous Moving Medium," *The Journal of the Acoustical Society of America*, Vol. 51, Number 5 (Part 2), 1972, pp. 1675 – 1682.

6. Ugincius, P. and Zondek, B., *Acoustic Rays in an Arbitrary Inhomogeneous Moving Medium*, U. S. Naval Weapons Laboratory Report No. TR-2446, Aug 1970.

7. Gholson, Norman H., *Evaluation and Utilization of the NWL Sound Intensity Prediction System,* NWL Technical Note TN-T-4/74, NSWCDD, Dahlgren, VA, Oct 1974.

8. Prater, L. L., *Gun Blast Far Field Peak Overpressure Contours*, NSWC TR-442, NSWCDD, Dahlgren, VA, Mar 1981.

9. Yagla, J. J., *Far Propagation of Blast From the 16-In. Naval Gun,* NSWC TR-86-191, NSWCDD, Dahlgren, VA, Dec 1986.

10. Lorenz, R. A., *Noise Abatement Investigation for the Bloodsworth Island Target Range: Description of Test Program and New Long Range Airblast Overpressure Prediction Method*, NSWC TR-81-431, NSWCDD, Dahlgren, VA, Nov 1981.

11. Lorenz, R. A., *Noise Abatement Investigation for the Bloodsworth Island Target Range: Data Report*, NSWC TR-81-433, NSWCDD, Dahlgren, VA, Nov 1982.

12. Pater, L. L., *FarField Overpressures from TNT Explosions: A Survey of Available Models*, NSWC TR 81-132, NSWCDD, Dahlgren, VA, Apr 1981.

REFERENCES (Continued)

13. Pollet, D. A., *Sound Intensity Prediction System for the Island of Kahoolawe; Program Maintenance Manual,* NSWC/DL TR-3786, NSWCDD, Dahlgren, VA, Mar 1978.

14. Kang, Sang-Wook and Kleiber, John C., Jr., *Atmospheric Propagation of High-Explosive Blast Waves,* Report UCRL-LR-1066330, Lawrence Livermore National Laboratory, University of California, Livermore, CA, Apr 1991.

15. Reed, J., *Explosion Airblast Predictions on a Personal Computer and Application to the Henderson, Nevada, Incident*, Report SAND 88-0681C Sandia National Laboratories, Albuquerque, NM, 1988.

16. Digital Terrain Elevation Data (DTED) Level 1 Coverage, Edition 3, Dated: 20 Jul 1995, The National Imagery and Mapping Agency, Fairfax, VA.

17 Kordich, M. M. and Pollet, D. A., *UTTR Noise Abatement 1995-1996 Data Version 1.01.14,* NSWCDD TR-97/148, NSWCDD, Dahlgren, VA, Jun 1997.

18. Irvin, J. et al., *Sound Studies of Open Burn and Open Detonation at Utah Test and Training Range*, Dames & Moore, Salt Lake City, UT, Jaycor, San Diego, CA, Sep 1997.

19. Radian International LLC, *Resource Conservation and Recovery Act Part B Permit Application for Open Burning/Open Detonation at the Utah Test and Training Range-North Thermal Treatment Unit*, Air Force Materiel Command, Hill Air Force Base, Utah, 1997.

DISTRIBUTION

	Copies
DOD ACTIVITIES (CONUS)	
ATTN CODE A76	
(TECHNICAL LIBRARY)	1
COMMANDING OFFICER CSSDD NSWC 6703 W HIGHWAY 98 PANAMA CITY FL 32407-7001	
DEFENSE TECH INFORMATION CTR 8725 JOHN J KINGMAN RD SUITE 0944 FORT BELVOIR VA 22060-6218	2
ATTN DR L L PATER	1
US ARMY CONSTRUCTION ENGRG RESEARCH LABORATORY P O BOX 4005 CHAMPAIGN IL 61824-4005	
ATTN CODE 00 ALC EME L HILL	1
CODE 00 ALC EME J WATKINS	1
CODE 75 OSS OSW CAPT FALVEY	1
HILL AIR FORCE BASE 7274 WARDLEIGH RD HILL AFB UT 84056-5137	
ATTN CODE 00 AL SUE R SHORT	1
ATTN CODE 00 AL SE T OLSEN	1
UTAH TEST AND TRAINING RANGE 75TH SQUADRON HILL AFB UT 84406	
ATTN CODE 950T M SWISDAK	6
CODE PM4A C PAINTER	1
COMMANDING OFFICER INDIAN HEAD DIVISION NSWC 101 STRAUSS AVE INDIAN HEAD MD 20640-5035	

	Copies
ATTN G LONG BLDG 79	3
SIERRA ARMY DEPOT HERLONG CA 96113-5000	
ATTN CODE 27432 W HELMRICH	1
DIRECTOR STRATEGIC SYSTEM PROGRAM 1931 JEFFERSON DAVIS HWY ARLINGTON VA 22241-5362	
ATTN CODE 521410D T WALTERS	1
COMMANDER NAWCWPNS CHINA LAKE CA	
ATTN T MOSKIOS BLDG E107	1
NASA WFF WALLOPS ISLAND VA 23337	
COMMANDING GENERAL MARINE CORPS COMBAT DEVELOPMENT COMMAND 3300 RUSSELL ROAD SUITE 227 QUANTICO VA 22134-5000	1
COMMANDING GENERAL MARINE CORPS BASE QUANTICO QUANTICO VA 22134-5000	1
COMMANDER FORT A P HILL BOWLING GREEN VA 22427-5000	1
ATTN AMSTE TM O	1
COMMANDER US ARMY TEST AND EVALUATION COMMAND ABERDEEN PROVING GROUND MD 21005-5055	

DISTRIBUTION (Continued)

	Copies
DOD ACTIVITIES (EX-CONUS)	
ATTN CODE 30 OPERATIONS	1
CODE 70 CHIEF ENGINEER	1
ATLANTIC FLEET WEAPONS TRAINING FACILITY NAVAL STATION ROOSEVELT ROADS PUERTO RICO	
NON-DOD ACTIVITIES (CONUS)	
THE CNA CORPORATION P O BOX 16268 ALEXANDRIA VA 22302-0268	1
ATTN CODE L 140 SANG WOOK KANG	1
LAWRENCE LIVERMORE NATIONAL LAB UNIVERSITY OF CALIFORNIA LIVERMORE CA 94551	
ATTN DR PHILEMON CHAN	1
JAYCOR 9775 TOWNE CENTRE DRIVE P O BOX 85154 SAN DIEGO CA 92186-5154	
ATTN R MITCHELL	3
B DICKSON	1
J NELSON	1
COMPUTER SCIENCES CORP UTAH TEST & TRAINING RANGE P O BOX 217 CLEARFIELD UT 84056	
ATTN K SEXTON	1
RADIAN INTERNATIONAL LLC 1093 COMMERCE PARK DR SUITE 100 OAK RIDGE TN 37830-8029	
ATTN M DELORETTO	1
RADIAN INTERNATIONAL LLC 4021 SOUTH 700 EAST SUITE 600 SALT LAKE CITY UT 84107	

		Copies
INTERNAL		
B60		3
G60	(WALTERS)	1
G63	(CARDWELL)	1
G72	(FILE)	10
G72	(KORDICH)	10
G72	(POLLET)	10